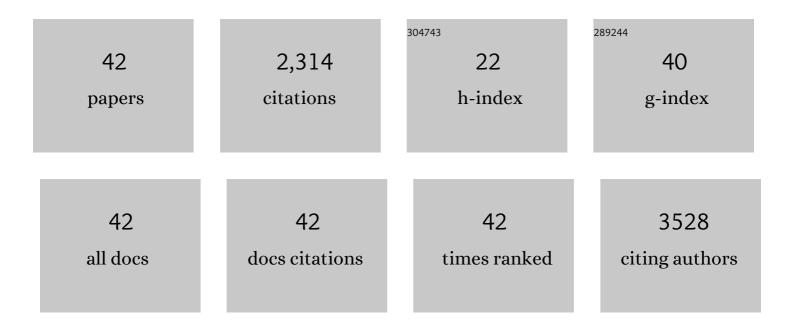
## **Zhiming Liu**

List of Publications by Year in descending order

Source: https://exaly.com/author-pdf/1525355/publications.pdf Version: 2024-02-01



#	Article	IF	CITATIONS
1	Iron-chalcogenide-based electrode materials for electrochemical energy storage. Journal of Materials Chemistry A, 2022, 10, 7517-7556.	10.3	20
2	Improving the chemical stability of blue heteroleptic iridium emitter FIrpic in the lowest triplet state through ancillary ligand modification: a theoretical perspective. Physical Chemistry Chemical Physics, 2022, 24, 9543-9550.	2.8	5
3	Tetrafunctional template-assisted strategy to preciously construct co-doped Sb@C nanofiber with longitudinal tunnels for ultralong-life and high-rate sodium storage. Energy Storage Materials, 2022, 48, 90-100.	18.0	27
4	NIR-II Responsive Molybdenum Dioxide Nanosystem Manipulating Cellular Immunogenicity for Enhanced Tumor Photoimmunotherapy. Nano Letters, 2022, 22, 4741-4749.	9.1	21
5	Oxygenated P/N co-doped carbon for efficient 2e <sup>â^'</sup> oxygen reduction to H <sub>2</sub> O <sub>2</sub> . Journal of Materials Chemistry A, 2022, 10, 14355-14363.	10.3	22
6	Redox responsive nanoparticle encapsulating black phosphorus quantum dots for cancer theranostics. Bioactive Materials, 2021, 6, 655-665.	15.6	56
7	Dual-responsive ultrathin 1T-phase niobium telluride nanosheet-based delivery systems for enhanced chemo-photothermal therapy. Journal of Materials Chemistry B, 2021, 9, 8109-8120.	5.8	11
8	Experimental investigation on the micro-morphologies and growing process of methane hydrate formation in SDS solution. Fuel, 2021, 293, 120320.	6.4	31
9	Influence of the Particle Size of Porous Media on the Formation of Natural Gas Hydrate: A Review. Energy & Fuels, 2021, 35, 11640-11664.	5.1	39
10	Investigation on Hydrate Formation and Growth Characteristics in Dissolved Asphaltene-Containing Water-In-Oil Emulsion. Langmuir, 2021, 37, 11072-11083.	3.5	17
11	A flexible Mn <sub>0.5</sub> Ti <sub>2</sub> (PO <sub>4</sub> ) <sub>3</sub> /C nanofiber film with superior cycling stability for potassium-ion batteries. Nanoscale, 2021, 13, 19956-19965.	5.6	9
12	SERS analysis of carcinoma-associated fibroblasts in a tumor microenvironment based on targeted 2D nanosheets. Nanoscale, 2020, 12, 2133-2141.	5.6	20
13	Effect of porous media and its distribution on methane hydrate formation in the presence of surfactant. Applied Energy, 2020, 261, 114373.	10.1	58
14	Wax and Wax–Hydrate Deposition Characteristics in Single-, Two-, and Three-Phase Pipelines: A Review. Energy & Fuels, 2020, 34, 13350-13368.	5.1	27
15	Few-Layer NbTe <sub>2</sub> Nanosheets as Substrates for Surface-Enhanced Raman Scattering Analysis. ACS Applied Nano Materials, 2020, 3, 11363-11371.	5.0	17
16	Rapid label-free SERS detection of foodborne pathogenic bacteria based on hafnium ditelluride-Au nanocomposites. Journal of Innovative Optical Health Sciences, 2020, 13, .	1.0	15
17	Photo-induced synthesis of molybdenum oxide quantum dots for surface-enhanced Raman scattering and photothermal therapy. Journal of Materials Chemistry B, 2020, 8, 1040-1048.	5.8	28
18	In situ photothermal activation of necroptosis potentiates black phosphorus-mediated cancer photo-immunotherapy. Chemical Engineering Journal, 2020, 394, 124314.	12.7	66

Zhiming Liu

#	Article	IF	CITATIONS
19	Rationally designed nitrogen-doped yolk-shell Fe7Se8/Carbon nanoboxes with enhanced sodium storage in half/full cells. Carbon, 2020, 166, 175-182.	10.3	39
20	Facile synthesis of metal-phenolic-coated gold nanocuboids for surface-enhanced Raman scattering. Applied Optics, 2020, 59, 6124.	1.8	3
21	Molybdenum oxide nano-dumplings with excellent stability for photothermal cancer therapy and as a controlled release hydrogel. New Journal of Chemistry, 2019, 43, 14281-14290.	2.8	14
22	Black phosphorus-Au filter paper-based three-dimensional SERS substrate for rapid detection of foodborne bacteria. Applied Surface Science, 2019, 497, 143825.	6.1	40
23	Black phosphorus–polypyrrole nanocomposites for high-performance photothermal cancer therapy. New Journal of Chemistry, 2019, 43, 8620-8626.	2.8	12
24	Facile hot spots assembly on molybdenum oxide nanosheets via in situ decoration with gold nanoparticles. Applied Surface Science, 2019, 480, 1162-1170.	6.1	21
25	Full-Scale Label-Free Surface-Enhanced Raman Scattering Analysis of Mouse Brain Using a Black Phosphorus-Based Two-Dimensional Nanoprobe. Applied Sciences (Switzerland), 2019, 9, 398.	2.5	10
26	Phase-controlled synthesis of molybdenum oxide nanoparticles for surface enhanced Raman scattering and photothermal therapy. Nanoscale, 2018, 10, 5997-6004.	5.6	85
27	Effect of Porous Media and Sodium Dodecyl Sulphate Complex System on Methane Hydrate Formation. Energy & Fuels, 2018, 32, 5736-5749.	5.1	48
28	Sb-based electrode materials for rechargeable batteries. Journal of Materials Chemistry A, 2018, 6, 8159-8193.	10.3	95
29	Electrochemical Energy Conversion and Storage with Zeolitic Imidazolate Framework Derived Materials: A Perspective. ChemElectroChem, 2018, 5, 3571-3588.	3.4	46
30	A two-dimensional fingerprint nanoprobe based on black phosphorus for bio-SERS analysis and chemo-photothermal therapy. Nanoscale, 2018, 10, 18795-18804.	5.6	86
31	Effect of silica sand size and saturation on methane hydrate formation in the presence of SDS. Journal of Natural Gas Science and Engineering, 2018, 56, 266-280.	4.4	69
32	Facile Fabrication of Flowerâ€Like C@ <i>α</i> â€Mo <sub>2</sub> C Hybrids with Enhanced Energy Storage Properties. ChemistrySelect, 2018, 3, 8395-8401.	1.5	0
33	Highly Graphitic Carbon Nanofibers Web as a Cathode Material for Lithium Oxygen Batteries. Applied Sciences (Switzerland), 2018, 8, 209.	2.5	7
34	Bi@C Nanoplates Derived from (BiO) <sub>2</sub> CO <sub>3</sub> as an Enhanced Electrode Material for Lithium/Sodiumâ€lon Batteries. ChemistrySelect, 2018, 3, 8973-8979.	1.5	23
35	A Nanoâ€Micro Hybrid Structure Composed of Fe <sub>7</sub> S <sub>8</sub> Nanoparticles Embedded in Nitrogenâ€Doped Porous Carbon Framework for Highâ€Performance Lithium/Sodiumâ€Ion Batteries. Particle and Particle Systems Characterization, 2018, 35, 1800163.	2.3	32
36	Synergistic protective effect of a BN-carbon separator for highly stable lithium sulfur batteries. NPG Asia Materials, 2017, 9, e375-e375.	7.9	85

Zhiming Liu

#	Article	IF	CITATIONS
37	Structure-designed synthesis of FeS <sub>2</sub> @C yolk–shell nanoboxes as a high-performance anode for sodium-ion batteries. Energy and Environmental Science, 2017, 10, 1576-1580.	30.8	475
38	Etchingâ€inâ€aâ€Box: A Novel Strategy to Synthesize Unique Yolkâ€5helled Fe <sub>3</sub> O <sub>4</sub> @Carbon with an Ultralong Cycling Life for Lithium Storage. Advanced Energy Materials, 2016, 6, 1502318.	19.5	158
39	Sb@C coaxial nanotubes as a superior long-life and high-rate anode for sodium ion batteries. Energy and Environmental Science, 2016, 9, 2314-2318.	30.8	414
40	Electrospun porous lithium manganese phosphate–carbon nanofibers as a cathode material for lithium ion batteries. Journal of Materials Chemistry A, 2015, 3, 17713-17720.	10.3	20
41	Electrospun Sn-doped LiTi <sub>2</sub> (PO <sub>4</sub> ) <sub>3</sub> /C nanofibers for ultra-fast charging and discharging. Journal of Materials Chemistry A, 2015, 3, 10395-10402.	10.3	43
42	Facile synthesis of Au@palladium oxide nano-sunflowers for ultrasensitive surface-enhanced Raman scattering analysis. New Journal of Chemistry, 0, , .	2.8	0